Journal Pre-proof

Statistical distribution of micro and macro pores in acrylic bone cement- effect of amount of antibiotic content

Mahsa Alimohammadi, Hassan Mirzabozorg, Farzam Farahmand, Sunjung Kim, Caroline Baril, Heidi-Lynn Ploeg

PII: S1751-6161(23)00651-3

DOI: https://doi.org/10.1016/j.jmbbm.2023.106297

Reference: JMBBM 106297

To appear in: *Journal of the Mechanical Behavior of Biomedical Materials*

Received Date: 10 July 2023

Revised Date: 2 September 2023

Accepted Date: 2 December 2023

Please cite this article as: Alimohammadi, M., Mirzabozorg, H., Farahmand, F., Kim, S., Baril, C., Ploeg, H.-L., Statistical distribution of micro and macro pores in acrylic bone cement- effect of amount of antibiotic content, *Journal of the Mechanical Behavior of Biomedical Materials* (2024), doi: https://doi.org/10.1016/j.jmbbm.2023.106297.

Pore Distribution

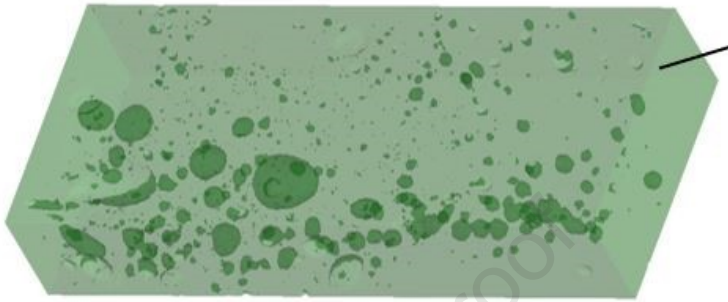

Three-parameter Weibull probability density functions

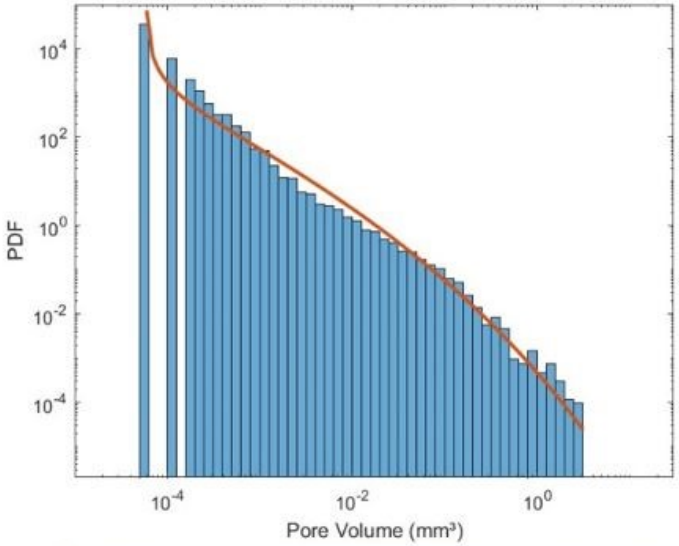

Statistical Analysis

Effect of antibiotic content

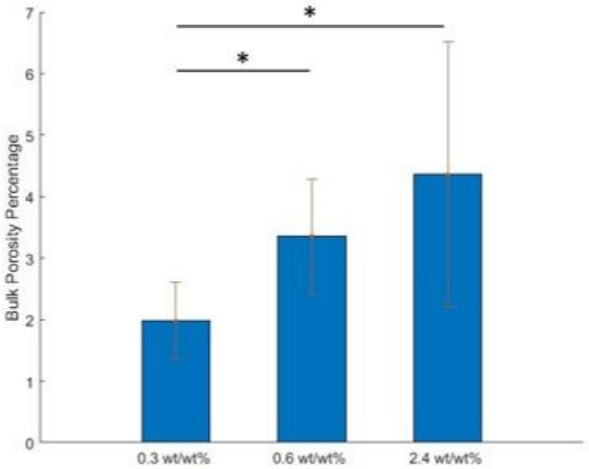

Enables developing probabilistic models of mechanical behavior

Explains the experimental fatigue test results

Statistical Distribution of Micro and Macro Pores in Acrylic Bone Cement-Effect of Amount of Antibiotic Content

Mahsa Alimohammadi[1,2], Hassan Mirzabozorg[1], Farzam Farahmand[3], Sunjung Kim[4], Caroline Baril[2], Heidi-Lynn Ploeg[2]

[1]Civil Engineering Department, KN Toosi University of Technology, Tehran, Iran

[2]Department of Mechanical and Materials Engineering, Queen's University, Kingston, ON, Canada

[3]Mechanical Engineering Department, Sharif University of Technology, Tehran, Iran

[4]Department of Orthopaedic Surgery, University of Illinois Chicago, Chicago, IL, USA.

Corresponding Author:

Heidi-Lynn Ploeg
Professor
Department of Mechanical and Materials Engineering, Queen's University at Kingston
McLaughlin Hall, Room 303B, 130 Stuart Street.
Kingston, ON, K7L 3N6
Canada
Email: heidi.ploeg@queensu.ca

Abstract

Aseptic loosening due to mechanical failure of bone cement is considered to be a leading cause of revision of joint replacement systems. Detailed quantified information on the number, size and distribution pattern of pores can help to obtain a deeper understanding of the bone cement's fatigue behavior. The objective of this study was to provide statistical descriptions for the pore distribution characteristics of laboratory bone cement specimens with different amounts of antibiotic contents. For four groups of bone cement (Palacos) specimens, containing 0.3, 0.6, 1.2 and 2.4 wt/wt% of telavancin antibiotic, seven samples per group were micro computed tomography scanned (38.97 μm voxel size). The images were first preprocessed in Mimics and then analyzed in Dragonfly, with the level of threshold being set such that single-pixel pores become visible. The normalized pore volume data of the specimens were then used to extract the logarithmic histograms of the pore densities for antibiotic groups, as well as their three-parameter Weibull probability density functions. Statistical comparison of the pore distribution data of the antibiotic groups using the Mann–Whitney non-parametric test revealed a significantly larger porosity ($p<0.05$) in groups with larger added antibiotic contents (2.4 and 0.6 wt/wt% vs 0.3 wt/wt%). Further analysis revealed that this effect was associated with the significantly larger frequency of micropores of 0.1 to 0.5 mm diameter ($p<0.05$) in groups with larger antibiotic content (2.4 wt/wt% vs and 0.6 and 0.3 wt/wt%), implying that the elution of the added antibiotic produces micropores in this diameter range mainly. Based on this observation and the fatigue test results in the literature, it was suggested that micropore clusters have a detrimental effect on the mechanical properties of bone cement and play a major role in initiating fatigue cracks in highly antibiotic added specimens.

Keywords: Palacos bone cement; Telavancin antibiotic; Micro-CT; Dragonfly; Histogram; Three-parameter Weibull distribution

Introduction

Joint replacement implants are categorized into two main groups of cementless and cemented, where the first group are most suited for younger and more active patients, and the latter for older patients with poor-quality (e.g., osteoporotic) bone [1]. In cemented joint prostheses, the implant is fixed into the bone by means of polymethylmethacrylate (PMMA) bone cement which acts as a grout between the implant and the bone through mechanical micro-interlocks. In spite of the high success rate of the cemented joint replacements, they are reported to a have limited lifespan, particularly in younger patients; the 10 year survival of cemented hip replacement systems has been reported to be 92.2% in the age group 55 to 64 years and 93.6% in the age group 65 to 74 years [2]. A leading reason of joint replacement revision is aseptic loosening due to mechanical failure of the cement mantel, the bone-cement interface, or the implant-cement interface [3].

The mechanical strength of PMMA bone cement depends on several factors, including molecular weight, ratio of polymers and monomers, grain size, antibiotic elution, defects and voids [4]. In particular, bone cement always contains voids and pores of different sizes, which affect the bone cement mechanical strength substantially [5-13] . There are several sources for formation of pores within the cement mantel. Micropores (diameter < 1 mm) are produced mainly as a result of monomer evaporation during polymerization process, as well as elution of the added antibiotic [14]. Macropores (diameter > 1 mm), on the other hand, are induced mainly due to entrapment of the air during mixing the bone cement and its application to the surgery site [14]. The other sources of void formation are polymerization and thermal shrinkage of the cement during setting process, in relation to the increased density of the polymerized cement and its contraction on the cooling front, respectively, which can form large pores particularly at the cement-implant interface [15]. Nevertheless, large pores might be also be produced due to incomplete filling of the bone cavity and premature solidification of the cement [14].

Several laboratory studies have shown that pores and voids are detrimental to the mechanical strength of the bone cement. It has been demonstrated that reducing the porosity percentage (pores' volume fraction) of the bone cement by vacuum mixing and centrifuging techniques increases its compressive [6, 9, 11] and bending [5, 6, 13] strength significantly. Also, it has been shown that the pores can act as crack initiation and propagation sites [8, 12] and the low-

porosity bone cements exhibit improved fatigue strength in comparison with the high-porosity ones [7, 10].

Recent studies have shown that the bulk porosity percentage alone is not sufficient to describe the porosity characteristics of the bone cement in relation to its mechanical strength; more detailed information, i.e., the size, number and distribution pattern of pores, are required to explain the diversity of fatigue strength results in specimens with the same porosity percentage. Hosseinzadeh et al. [16] reported that the pores greater than a critical size can induce high stress concentrations and initiate fatigue cracks, while the small pores might work as crack arrestors. Also, Ishihara et al. [8], Cristofolini et al. [17] and Hoey et al. [14] found that the fatigue strength of bone cement is dramatically reduced as pore size increases, with macropores (diameter > 1 mm) being particularly damaging. In addition to the pore size, the distribution pattern of the pores, e.g., pores' collection and clusters, has been also reported to be critical since the fatigue failure may initiate by cracking between small pores in close proximity [10, 18-20]. This behavior has been well demonstrated by simulation of the damage accumulation in high density pore cluster areas of bone cement [21]. Also the finite element study of Hoey et al. [14] showed that a couple of pores in close proximity can form a large pore of complex shape and inevitably a higher stress concentration, initiating the complete failure of the material.

Considering the important role of the pores and voids on the mechanical and particularly the fatigue behavior, several studies have investigated the porosity characteristics of the bone cement using a variety of techniques. Traditionally, porosity has been investigated using high-resolution radiography for macropores and light microscopy for micropores [5, 7, 9, 13, 22-25]. For instance, Wang et al. [26] took radiographs from cement specimens, prepared with different vacuum levels and mixing methods, and measured the number, diameter, and volume percentage of the macropores, by calibrating the radiographs against that of a metal plate with holes of 1-10 mm. They also measured the number and surface density of micropores (0.1<diameter<1 mm) on the surfaces of sample slices cut from specimens using an optical microscope. In spite of the valuable information provided by these studies, they are limited to examining the porosity in two dimensions (2D). Hence, they cannot provide information on the nonhomogeneous three-dimensional (3D) distribution pattern of the pores. Moreover, the radiography-based measurement of the macropores is subjected to large errors since it superimposes the pores onto a 2D plan and provides a mottled image with no clear pore

boundaries [27]. Finally, the microscopic study of micropores can be performed on a limited number of planar sections only, rather than the whole bulk of the specimen.

In response to these limitations, recent studies have employed the micro-computed tomography (μ-CT) imaging technique which provides information from the 3D distribution of the pores in the cement specimens. Most studies, however, have only quantified the bulk porosity percentages of the bone cement specimens. For instance, in the work of Cox et al. [27] the porosity percentages of the bone cement specimens were measured using both μ-CT imaging and traditional techniques, and a poor agreement was found suggesting the insufficiency of the latter method. Also, in the works of Pithankuakul et al. [11] and Kim et al. [28] the porosity percentages of the bone cement specimens, prepared with different mixing speeds, times of antibiotic addition, and amounts of added antibiotic, were quantified and compared. Finally, in the work of Hoey et al. [14], the μ-CT images of the cement specimen, mixed either by hand or under vacuum, were used to provide 3-D visualizations of the porosity distributions. They reported that the hand-mixed specimens contained a large number of micropores with an even distribution while the vacuum-mixed specimens included fewer micropores but large singular macropores at the boundaries.

To provide a better understanding of the bone cement behavior during mechanical experiments, there is a need for quantified detailed information on the number, size and distribution pattern of the pores in the laboratory specimens. This is particularly true for the antibiotic added bone cement, where the mechanical properties, including the compressive strength [29-43], flexural strength [32-34, 37, 39, 40, 42-45], fracture toughness [39, 42, 44] , and fatigue resistance [33, 46] , are largely affected by the amount of the antibiotic. This effect is often attributed to the increased porosity of the antibiotic added bone cement due to antibiotic elution, as shown in previous studies [42, 44]. However, the mechanism through which the antibiotic elusion induced porosity influences the mechanical strength is still unknown.

Moreover, several studies [8, 14, 16, 17, 28] have suggested that the controversial results of the fatigue experiments on cement specimens might be only explained in view of detailed data on the number, size, and 3D distribution pattern of pores. Previous modeling studies [14, 21, 28] have also emphasized that such data is critical for more realistic model predictions, particularly for developing sophisticated probabilistic models of the bone cement's mechanical behavior, as has been conducted for biological tissues [47]. The objective of this study was to analyze the μ-CT images of laboratory bone cement specimens using advanced image

processing techniques, in order to provide detailed statistical data of pores' distribution. More specifically, it was intended to compare the number, size and distribution pattern of pores in bone cement specimens with different amounts of antibiotic contents to help a better understating of the strength deteriorating mechanism of antibiotic elusion.

Methods

In order to study the porosity of laboratory bone cement specimens, samples from a previously published study [28] were examined. Here a brief description of the material preparation and imaging protocols is provided. Four groups of bone cement (Palacos®R) specimens, containing 0.3, 0.6, 1.2 and 2.4 wt/wt% of telavancin antibiotic (Theravance Biopharma US, Inc., CA, USA) were prepared. First, 40 g of cement powder and telavancin were hand mixed in a syringe for 1 min and then the blended powder and the cement liquid were vacuum mixed (-5 kPa). The mixture was then poured into a semi-open aluminum mold to form a prismatic specimen with dimensions of 44 mm length, 5 mm width and 10 mm height with fabricated 5 mm cracks at the middle of their lengths according to ASTM-D5045 for plane strain fracture toughness tests. The specimens were cured in 1×PBS for 21 days at 21℃ and then subjected to fracture toughness testing. After mechanical testing, the broken specimen halves, with approximate dimensions of 22 mm length, 5 mm width and 10 mm height (Figure 1) were scanned eight at a time using a μ-CT system (MicroXCT400, Xradia, Oberkochen, Germany), with X-ray tube setting of 80 kV, 9 W and 100 μA, exposure time of 0.5 s, and frame averaging of 100. For each specimen, 400 2D-image slices were obtained with 40 mm fields of view and 38.97 μm pixel size and thickness. The total scan time per sample was approximately 1 hour. Seven half samples per antibiotic group were imaged.

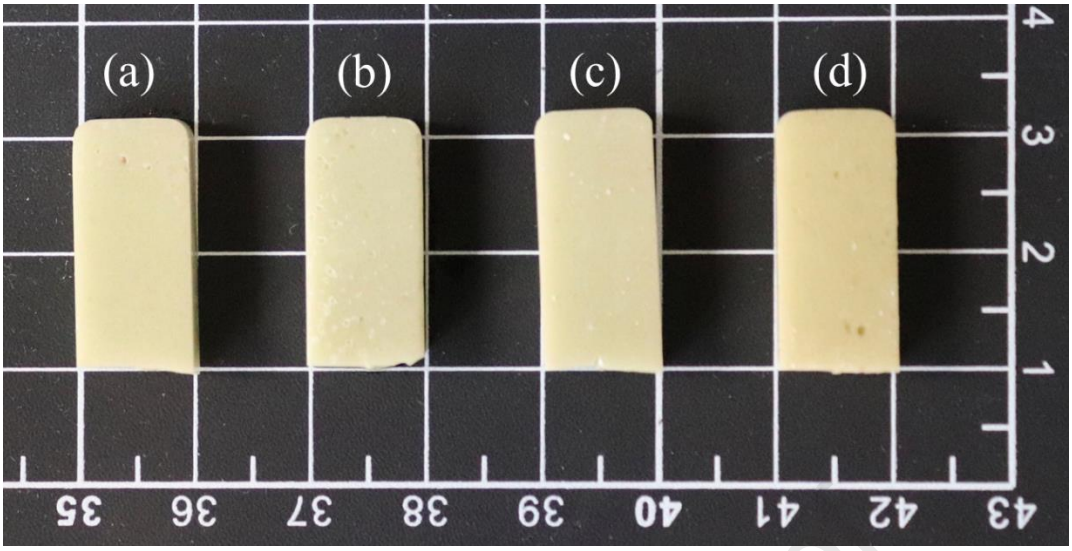

Figure 1. Bone cement material test specimen halves containing (a) 0.3, (b) 0.6, (c) 1.2 and (d) 2.4 wt/wt% of antibiotic.

The μ-CT images of the material test specimen halves were first preprocessed in Mimics (Innovation Suite 24.0, Materialise NV, Leuven, Belgium). Two masks were created to increase the image contrast and improve the pore visualization; a dark mask was applied to the whole bulk of the bone cement specimen and a brighter one to the pore-contained bone cement (Figure 2). For each specimen, the threshold of the latter mask was systemically changed by the operator to reach a state in which a considerable number of single-pixel pores appeared simultaneously; both a lower and a higher threshold level would result in a larger number of multiple-pixel pores than the single-pixel ones. This method enabled correction of the partial volume effect, to some extent, and detection of the micropores with very small sizes.

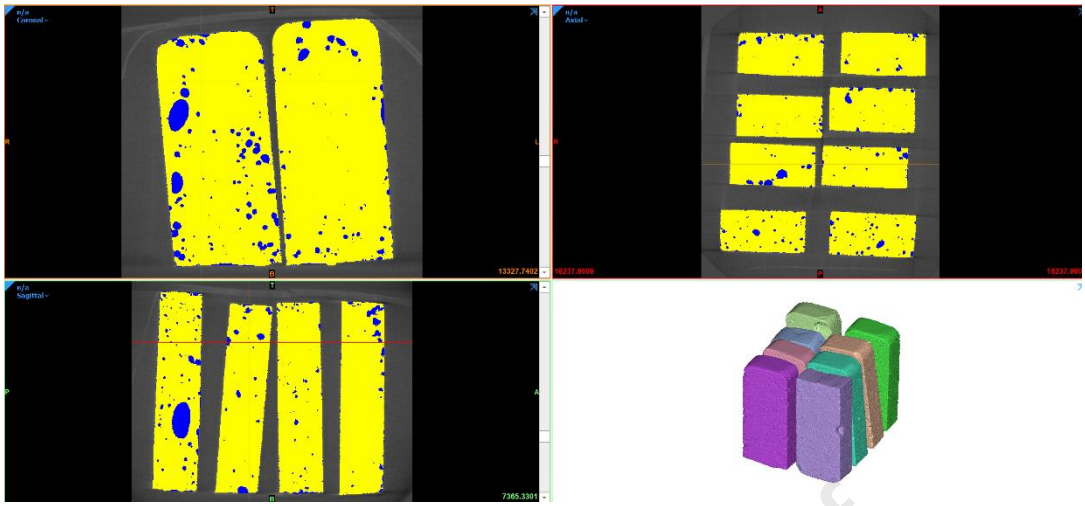

Figure 2. Preprocessing of μ-CT images in Mimics (Materialise NV, Leuven, Belgium). A dark mask was applied to the whole bulk of the bone cement specimen and a brighter one to the pore-contained bone cement.

The μ-CT images were imported into Dragonfly (version 2021.1.0.977, Object Research Systems, Montreal, Canada) for further processing and analysis. First, internal prismatic volumes of interest, with a mean volume of 476.70± 0.87 mm^3, were defined to exclude surface effects (Figure 3.a). Then, for each slice within the region of interest, the pores were segmented automatically based on the thresholding performed in Mimics. The 3D models of the specimens containing volumetric pores were reconstrued for visualization (Figure 3.b) and the adjacent pores were examined carefully to join those with a single voxel interface manually.

(a) (b)

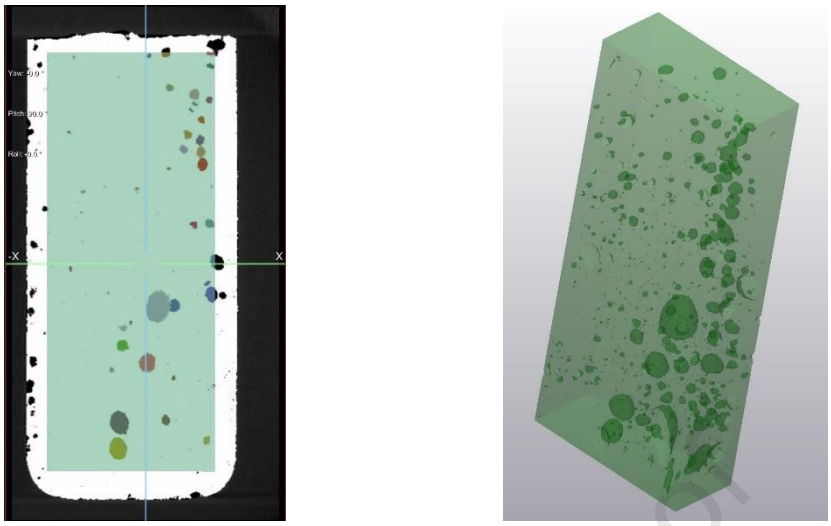

Figure 3. Processing of μ-CT images in Dragonfly (Object Research Systems, Montreal, Canada). (a) μ-CT slice of a specimen with region of interest shown in green color, (b) 3D rendered model of the specimen.

The 3D models were analyzed in Dragonfly to quantify the pore distribution parameters in the bone cement specimens. For each specimen, pores with volumes larger than that of a single voxel (5.92E-05 mm^3) were identified and their volumes were recorded. Then for each antibiotic group, the densities of different pore volumes were found by normalizing the pore volume frequency data across the seven specimens of that group to their total bulk volume. The results were then imported to MATLAB (R2022b, MathWorks, Natick, Massachusetts) to be illustrated as logarithmic histograms of the pore densities. MATLAB was also used to fit three-parameter Weibull probability density functions (PDF) to the pore distribution data (1):

$$f(x|a,b,c) = \begin{cases} \frac{b}{a}\left(\frac{x-c}{a}\right)^{b-1} exp\left(-\left(\frac{x-c}{a}\right)^{b}\right) & if\ x > c, \\ 0 & if\ x \le c, \end{cases} \quad (1)$$

where a, b and c are the scale, shape and location parameters of the PDF, respectively, x is a pore volume in mm^3 and $f(x|a,b,c)$ represents the probability density of x.

In order to compare the porosity distribution characteristics of different antibiotic groups, some descriptive statistics were also calculated. The porosity percentages of the specimens of each group, found by dividing the total pore volume of each specimen to its bulk volume, were

averaged to obtain the bulk porosity percentage of each group. Also, averaged pore size distribution bar graphs were produced for each group, based on the pore diameters. First, an equivalent diameter was found for each pore by calculating the diameter of a sphere with the same volume. Pores with diameters smaller than 1 mm were considered as micropores, and those with diameter between 1 mm and 3 mm as macropores. Pores with diameters larger than 3 mm were considered to be produced due to cementing deficiency and were excluded from the analysis. The diameter bins were defined in ranges of 0.01 to 0.05 mm, 0.05 to 0.1 mm, 0.1 to 0.5 mm, and 0.5 to 1 mm for the micropores, and 1 to 1.5 mm, 1.5 to 2.0 mm, 2.0 to 2.5 mm, and 2.5 to 3.0 mm for the macropores. For each antibiotic group, the pore diameter frequency data were averaged and the means and the standard deviations of the pore densities of different diameter bins were found and compared.

Statistical comparisons were performed in MATLAB environment. The Kolmogorov-Smirnov test showed a non-normal distribution of the data across samples, which was not unexpected considering the small number of specimens of each group. The Mann–Whitney non-parametric test was hence used to compare the effect of the amount of the added antibiotic on the average-based distributions parameters of pores, considering the significance level set to $p<0.05$.

Results

Examination of the μ-CT data showed that the images of the 1.2 wt/wt% added antibiotic specimens were blurred and insufficient for detecting pores of the minimum sizes (diameter range of 0.01 to 0.1 mm). Hence, this group was excluded from further analysis. The logarithmic histograms of the other groups of study (0.3, 0.6 and 2.4 wt/wt% of added antibiotic) are shown in Figure 4. A singular pore of excessive large size (> 3mm diameter) was observed in one specimen of the 2.4 wt/wt% group. The three-parameter Weibull probability density functions, with the parameters indicated in Table 1, provided reasonable fits with the pore distribution data.

Table 1- Parameters of the three-parameter Weibull probability density functions for bone cement specimens of different antibiotic groups.

Group of Specimens	*a*	*b*	*c*
0.3 wt/wt% added antibiotic	2.32E-05	0.1962	5.92E-05
0.6 wt/wt% added antibiotic	2.48E-05	0.1776	5.92E-05
2.4 wt/wt% added antibiotic	1.40E-03	0.3643	5.92E-05

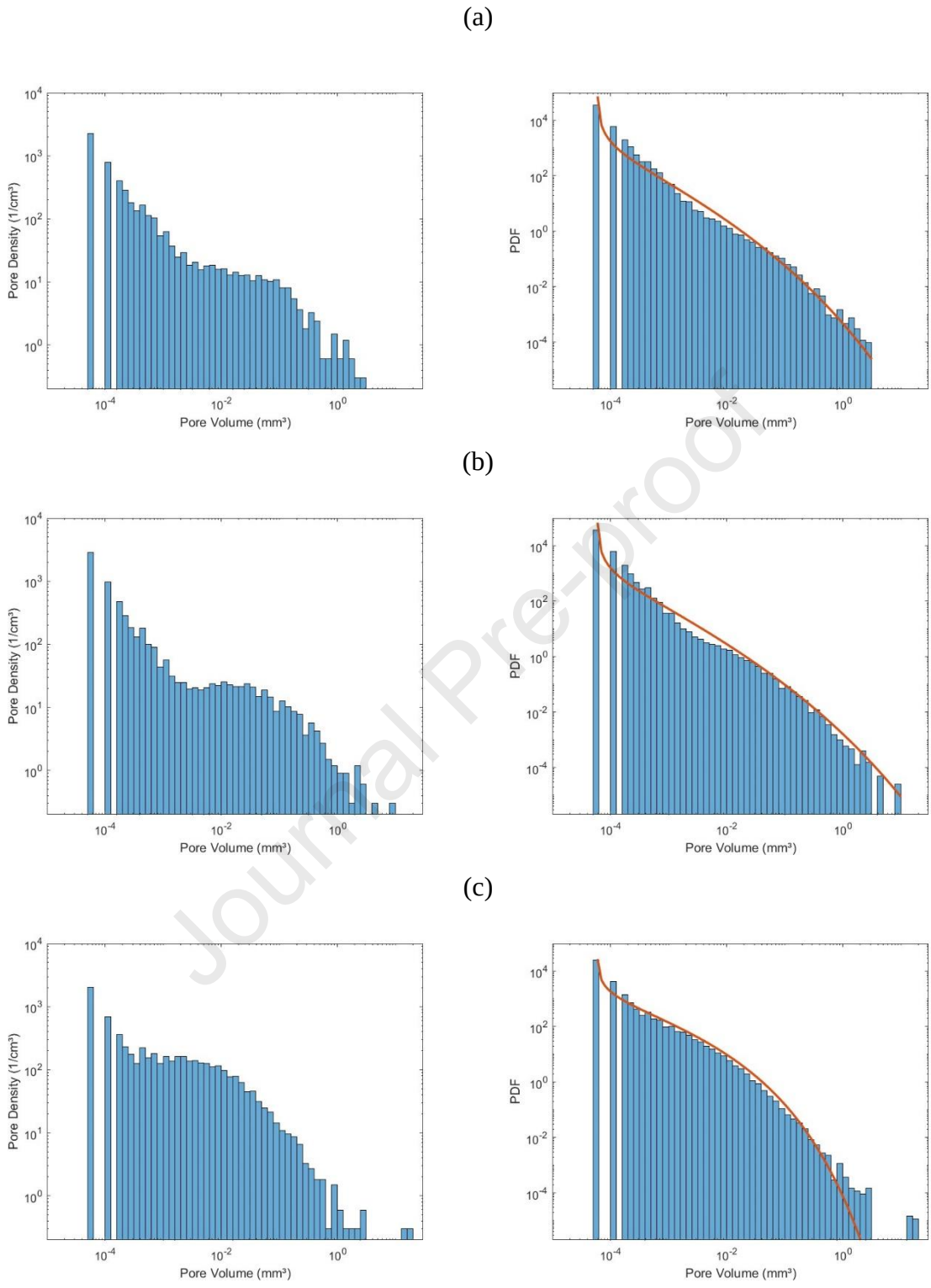

Figure 4. Logarithmic histograms (Left) and probability densities (Right) of the pore volumes in cement specimens containing (a) 0.3, (b) 0.6, and (c) 2.4 wt/wt% added antibiotic. The red curves show the Weibull probability density functions (parameters in Tables 1).

The means and standard deviations of the porosity percentages of the specimens of different antibiotic groups are shown in Figure 5. The porosity percentage which was 2.0±0.63% for the 0.3 wt/wt% group increased significantly to 3.4±0.93 % for the 0.6 wt/wt% and to 4.4±2.16% for the 2.4 wt/wt% groups ($p<0.05$). The difference of the porosity percentages of the 0.6 wt/wt% and the 2.4 wt/wt% groups was not statistically significant.

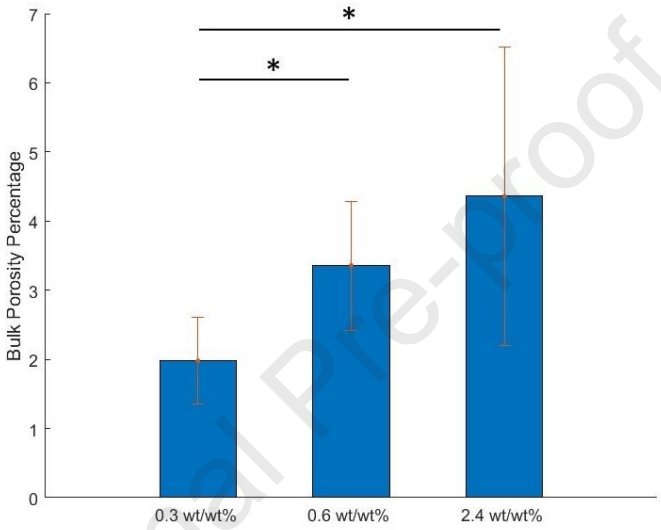

Figure 5. The means and the standard deviations of the bulk porosity percentages of the specimens of different antibiotic groups. Asterisks (*) denotes a significant statistical difference ($p<0.05$).

The means and standard deviations of the averaged pore-size distributions data across specimens of each of the 0.3, 0.6 and 2.4 wt/wt% added antibiotic groups are illustrated in Figure 6. In general, the density of small micropores (diameter <0.1 mm) was consistently large in all groups; between 2000/cm^3 and 2900/cm^3 for pores of 0.01-0.05 mm diameter, and 1800/cm^3 and 2300/cm^3 for pores of 0.05-0.1 mm diameter. However, the volume fraction of these pores was very small (less than 0.05% in total). For micropores of 0.1-0.5 mm diameter, both the density and the volume fraction were considerable in all groups. However, the pore density data indicated significantly smaller pore frequencies in the 0.3 and 0.6 wt/wt% added antibiotic groups (means: 637±214/cm^3 and 668±137/cm^3, respectively) than in the 2.4 wt/wt%

group (mean: 2304±280/cm^3), ($p<0.05$) (Figure 7.a). A similar observation was also made for the resulting volume fractions, with significantly smaller values for the 0.3 and 0.6 wt/wt% added antibiotic groups (means: 0.38±0.13% and 0.57±0.13%, respectively), than the 2.4 wt/wt% group (mean: 1.63±0.48%), ($p<0.05$) (Figure 7b). The micropores of 0.5-1.0 mm had a limited frequency of up to 75/cm^3 in maximum, with no significant difference between the groups. The volume fractions of this diameter range in the 0.3, 0.6 and 2.4 wt/wt% groups were respectively 0.82±0.24%, 1.28±0.41%, and 1.07±0.50%, where only the difference between the first two groups was significant ($p<0.05$).

The frequency of macropores was rather small in the specimens, with the densities between 4.5/cm^3 and 7.5/cm^3 for 1-1.5 mm diameter pores, and 0.9/cm^3 and 2.1/cm^3 for 1.5-2.0 mm diameter pores. Also, the volume fractions were relatively similar (range: 0.37±0.23% to 0.64±0.45% for 1-1.5 mm diameter and 0.21±0.36% to 0.55±0.41% for 1.5-2 mm diameter pores). Larger macropores (> 2mm diameter) were only observed as singular pores in the 0.6 and 2.4 wt/wt% added antibiotic groups. Statistical comparison of the results of different groups revealed no significant effect for the amount of added antibiotic.

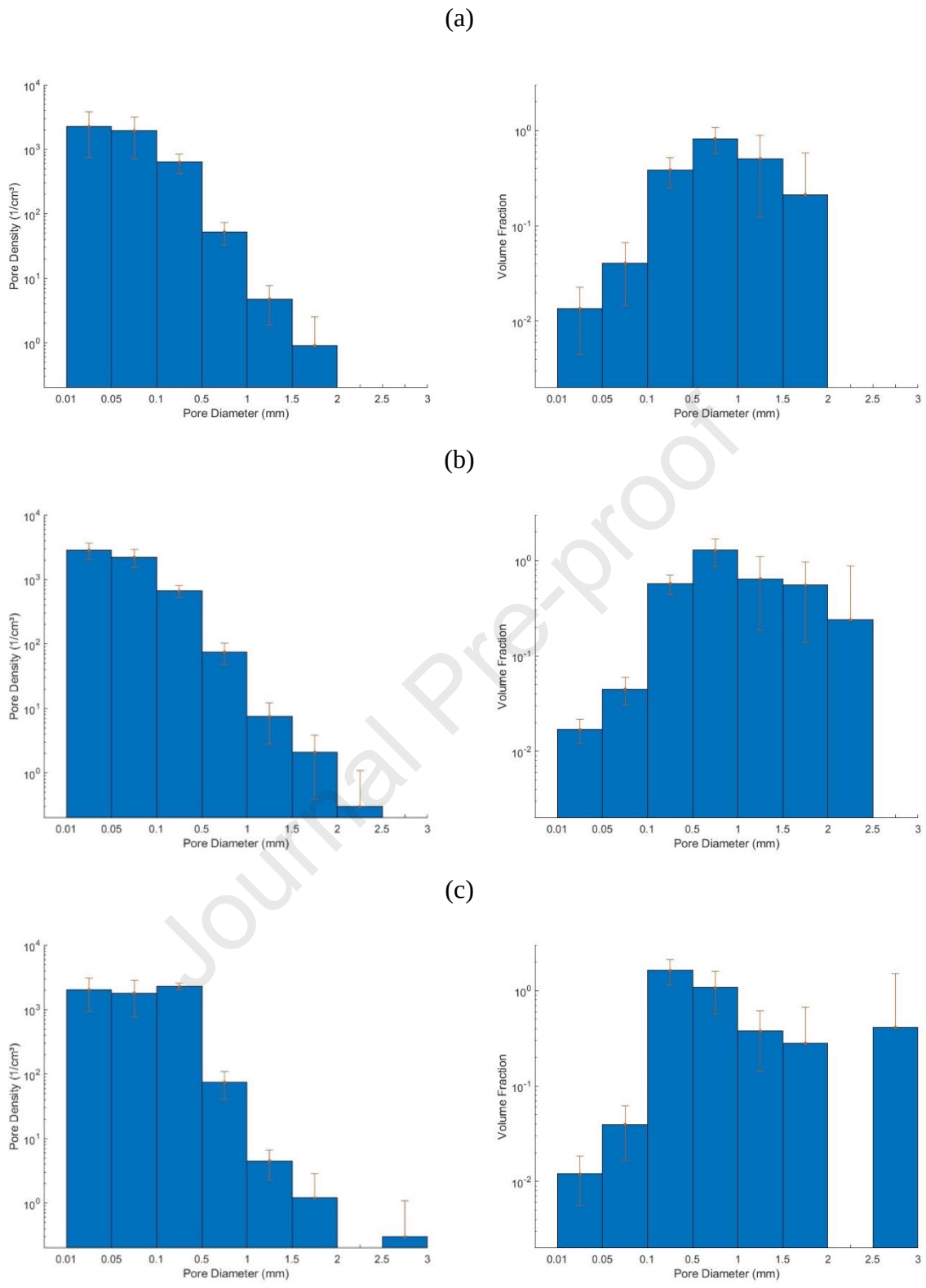

Figure 6. Means and standard deviations of the averaged pore-size distributions data across specimens of each of (a)0.3, (b) 0.6, and (c) 2.4 wt/wt% added antibiotic groups.

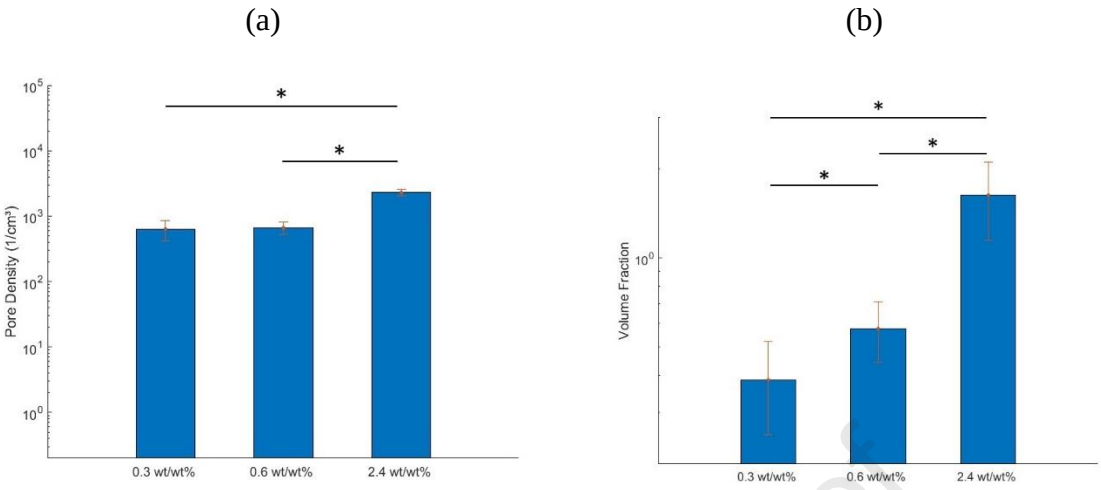

Figure 7. Means and standard deviations of the (a) densities and (b) volume fractions of micropores of 0.1-0.5 mm diameter across specimens of 0.3, 0.6, and 2.4 wt/wt% added antibiotic groups. Asterisks (*) denotes a significant statistical difference ($p < 0.05$).

Discussion

The failure of the cemented joint replacement systems is often attributed to the fatigue failure of the cement mantle, the bone-cement interface, or the implant-cement interface, leading to aseptic implant loosening [3]. Considering the important effect of the pores on the fatigue behavior of the bone cement [5-13], this study investigated the number, size and distribution pattern of the pores in the material test specimens using μ-CT imaging. In particular, by employing advanced image processing techniques, we could detect micropores of small sizes which have been often neglected in previous studies [5, 7, 9, 13, 14, 22-27]. Although large pores are often considered to be responsible for inducing high stress concentrations and initiating the fatigue cracks [8, 16, 17], recent studies [10, 14, 21] have reported that small micropores might be equally critical when they are in close proximity and act as clusters.

Moreover, our study provided quantified detailed information on the distribution characteristics of pores, which can help understanding the behavior of bone cement specimens during fatigue experiments. The histograms of the pore densities and the associated probability density functions for different amounts of added antibiotic (Figure 4), as well as the averaged pore-size distributions data (Figure 6). These statistical data are essential for developing probabilistic models of the bone cement, in order to obtain more realistic predictions of its mechanical and failure behaviors.

The results of our study for the bulk porosity percentage of the bone cement specimens (Figure 5) are in general agreement with the previous reports. For instance, Macaulay et al. [48] found an average porosity of 1.62% for their vacuum-mixed non-antibiotic added specimens, which is comparable with our finding for the 0.3 wt/wt% added antibiotic group (2.0%). Also, Slane et al. [39] reported mean porosities in the range of 2.4% to 9.9% for their specimens with different amounts of the added antibiotic. Nevertheless, our bulk porosity results are smaller in comparison with those reported by Kim et al. [28] for the same specimens; this difference is thought to be due to the 3D image processing techniques employed in our study.

Based on our results for the bulk porosity percentage (Figure 5), a larger amount of added antibiotic was associated with a larger porosity in bone cement specimens. This effect was statistically significant ($p<0.05$) when comparing the 2.4 and 0.6 wt/wt% added antibiotic groups with the 0.3 wt/wt% group, but not between the 2.4 and 0.6 wt/wt% groups. This observation is in agreement with the previous studies which have reported increased porosity

[28, 42] and decreased mechanical strength [42] in the bone cement specimens with higher contents of the antibiotic.

An interesting finding of this study was the relationship between the added amount of the antibiotic and the pore-size distribution data (Figure 6). Our results indicated relatively similar averaged-based pore-size distributions for different amounts of the added antibiotic, except for the pores of 0.1 to 0.5 mm diameter (Figure 7). This finding indicates that the increased porosity percentage of the bone cement specimens due to the increased content of antibiotic is mainly due to the larger frequency of the 0.1 to 0.5 mm diameter micropores, and suggests that the elution of the added antibiotic produces micropores in this diameter range mainly. This observation is of great importance for interpretation of the fatigue test results of the bone cement specimens. Previous studies have often suggested that the decreased fracture strength of the bone cement specimens with higher amount of the added antibiotic was due to their larger number of macropores, greater than a critical size (typically 1 mm diameter) [8, 14, 17, 28]. Based on our results, it might be suggested that micropore clusters have a detrimental effect on the mechanical properties of bone cement and play a major role in initiating fatigue cracks in highly antibiotic added specimens. This finding is supported by the fatigue failure mechanism, proposed in previous modeling studies. In the work of Jeffers et al. [21], which simulated the damage accumulation process in bone cement, it was shown that damage is accumulated in pore cluster areas and can cause premature fatigue failure. Also, in the work of Hoey et al. [14], the effect of pore clusters in bone cement was analyzed using the theory of critical distances and it was shown the high local stresses between pores in close proximity can lead to in-between cracking at a very early stage. This cracking would essentially link the pores together, forming a pore of complex shape and inevitably a higher stress concentration, which initiates the complete failure of the material. These failure scenarios have been observed by fractography analysis using SEM which demonstrated a distribution of small pores with occasionally larger pores on the fracture surfaces, indicative of the pores interaction in forming crack initiation sites [10, 18-20].

The findings of this study highlight the importance of taking appropriate measures in clinical practice to avoid formation of antibiotic elusion induced pore clusters within bone cement, as much as possible. First of all, the amount of the added antibiotic should be kept as low as necessary to minimize the number of pores. Moreover, the antibiotic powder shall be incorporated into the cement powder such that a homogeneous dispersion of powders is

achieved. A uniform distribution of the antibiotic particles would help to prevent formation of antibiotic agglomerations and high-density pore clusters, i.e., pores in close proximity. Previous studies have reported that the mechanical properties of antibiotic added bone cement is improved when the powders are mixed using a turbo blender [49, 50].

This study suffers from some limitations which should be addressed in future investigations. In our setup, we employed a semi-open mold aluminum design with separated flat top and bottom plates, to create gaps that allow for gas release and pressure relief during bone cement polymerization. To ensure a precise fit and maintain consistent dimensions, we utilized clamps to securely hold the flat plates in place during the molding process. This effectively reduced the risk of void formation and ensured better control over the polymerization process. However, to compensate for the gaps, we added an extra 1-2mm thickness to the bone cement sample, which was later ground down to achieve the desired dimensions and surface finish. Despite this controlled fabrication method, it is essential to acknowledge that achieving a perfect elimination of voids might remain challenging. The polymerization process is complex, involving various chemical reactions, and achieving absolute uniformity in a solidifying material is difficult. Additionally, the presence of small air pockets or inconsistencies in the bone cement mixture might be difficult to eliminate completely, even with the semi-open molding and vacuum mold systems we used.

Moreover, the numbers of antibiotic groups and the specimens per group were limited in our study. This limitation was due to the fact that the specimens and their μ-CT data used in this study were obtained from a previous study [28]. The μ-CT data of the 1.2 wt/wt% group contained pixelated and blurry images, and unfortunately, the original samples had been discarded and were not available for rescanning. Also, the number of samples in the control group (0% added antibiotic) was three, with only two with good scan data. More comprehensive and statistically reliable data for the effect of the added antibiotic on the distribution of the pore densities and the associated probability density functions can be obtained in future by examining more antibiotic groups with larger number of specimens.

Furthermore, considering the partial volume effect, the smallest pore guaranteed to be detected in our study (in the worst-case scenario) was a cube of 2×2×2 voxels. With a pixel size of 38.97 μm, this cube would have a volume of 473E-3 mm^3 and an equivalent diameter of 96.70 μm. Hence, the number of micropores of smaller sizes reported in our study shall be regarded as an underestimation. Nevertheless, the methodology used in our study for setting the threshed level

corrected the partial volume effect, to some extent, and enabled detection of a very large number of single-voxel micropores (Figure 4). Future studies can provide more accurate results for small micropores by employing μ-CT machines with higher resolutions (smaller voxel sizes). Finally, our results are limited to one specific type of bone cement (Palacos®R) and antibiotic (Telavancin). For generalized conclusions, future investigations should consider other types of bone cements and antibiotic contents. This is also true for the radiopacifier (zirconium dioxide) content of Palacos®R. Although the radiopacifier particles have no direct effect on pore formation, they are reported to reside within the polymerization pores [51], which might affect the results of the pore distribution data captured using μ-CT. This effect, however, is thought to be negligible considering the small sizes of these particles (typical mean diameter of 1 to 2 μm [52]).

It was concluded that the elution of the added antibiotic produces micropores in the 0.1 to 0.5 mm diameter range mainly, which considering the fatigue test results in the literature, suggests that micropore clusters play a major role in initiating fatigue cracks in highly antibiotic added specimens.

Funding

During the course of this study, the first author was supported by grants from the Natural Sciences and Engineering Research Council of Canada (NSERC), and International Society of Biomechanics.

References

1. Zhang, C., C.H. Yan, and W. Zhang, *Cemented or cementless fixation for primary hip arthroplasty—evidence from The International Joint Replacement Registries.* Ann Joint, 2017. **2**(10): p. 57.
2. Mäkelä, K.T., et al., *Failure rate of cemented and uncemented total hip replacements: register study of combined Nordic database of four nations.* Bmj, 2014. **348**.
3. Jasty, M., et al., *The initiation of failure in cemented femoral components of hip arthroplasties.* The Journal of bone and joint surgery. British volume, 1991. **73**(4): p. 551-558.
4. Harper, E.J. and W. Bonfield, *Tensile characteristics of ten commercial acrylic bone cements.* Journal of biomedical materials research, 2000. **53**(5): p. 605-616.
5. Baleani, M., R. Fognani, and A. Toni, *The influence of stem insertion rate on the porosity of the cement mantle of hip joint replacements.* Proceedings of the

Institution of Mechanical Engineers, Part H: Journal of Engineering in Medicine, 2003. **217**(3): p. 199-205.
6. Dunne, N.J. and J.F. Orr, *Influence of mixing techniques on the physical properties of acrylic bone cement.* Biomaterials, 2001. **22**(13): p. 1819-1826.
7. Dunne, N.J., et al., *The relationship between porosity and fatigue characteristics of bone cements.* Biomaterials, 2003. **24**(2): p. 239-245.
8. Ishihara, S., et al., *On fatigue lifetimes and fatigue crack growth behavior of bone cement.* Journal of Materials Science: Materials in Medicine, 2000. **11**: p. 661-666.
9. Lewis, G., J.S. Nyman, and H.H. Trieu, *Effect of mixing method on selected properties of acrylic bone cement.* Journal of biomedical materials research, 1997. **38**(3): p. 221-228.
10. Murphy, B.P. and P.J. Prendergast, *On the magnitude and variability of the fatigue strength of acrylic bone cement.* International Journal of Fatigue, 2000. **22**(10): p. 855-864.
11. Pithankuakul, K.M.D., et al., *The Effects of Different Mixing Speeds on the Elution and Strength of High-Dose Antibiotic-Loaded Bone Cement Created With the Hand-Mixed Technique.* The Journal of arthroplasty, 2014. **30**(5): p. 858-863.
12. Sinnett-Jones, P.E., et al., *Crack initiation processes in acrylic bone cement.* Journal of Biomedical Materials Research Part A: An Official Journal of The Society for Biomaterials, The Japanese Society for Biomaterials, and The Australian Society for Biomaterials and the Korean Society for Biomaterials, 2009. **89**(4): p. 1088-1097.
13. Wilkinson, J.M., et al., *Effect of mixing technique on the properties of acrylic bone–cement: A comparison of syringe and bowl mixing systems.* The Journal of arthroplasty, 2000. **15**(5): p. 663-667.
14. Hoey, D. and D. Taylor, *Quantitative analysis of the effect of porosity on the fatigue strength of bone cement.* Acta biomaterialia, 2009. **5**(2): p. 719-726.
15. Gilbert, J.L., et al., *A theoretical and experimental analysis of polymerization shrinkage of bone cement: A potential major source of porosity.* Journal of biomedical materials research, 2000. **52**(1): p. 210-218.
16. Hosseinzadeh, H.R.S., et al., *The acrylic bone cement in arthroplasty.* Orthopedics, Physical Medicine and Rehabilitation, Edited by Plamen Kinov, 2013: p. 101-130.
17. Cristofolini, L., C. Minari, and M. Viceconti, *A methodology and criterion for acrylic bone cement fatigue tests.* Fatigue & Fracture of Engineering Materials & Structures, 2000. **23**(11): p. 953-957.
18. Hoey, D. and D. Taylor, *Fatigue in porous PMMA: The effect of stress concentrations.* International journal of fatigue, 2008. **30**(6): p. 989-995.
19. Browne, M., N. Shearwood-Porter, and I. Sinclair, *The role of microconstituents on the fatigue failure of bone cement.* Procedia engineering, 2018. **213**: p. 98-103.
20. Qu, G.-X., et al., *Mechanical Properties and Porosity of Acrylic Cement Bone Loaded with Alendronate Powder.* International journal of medical sciences, 2018. **15**(13): p. 1458-1465.
21. Jeffers, J.R.T., et al., *On the Importance of Considering Porosity When Simulating the Fatigue of Bone Cement.* Journal of biomechanical engineering, 2005. **127**(4): p. 563-570.
22. Smeds, S., D. Goertzen, and I. Ivarsson, *Influence of temperature and vacuum mixing on bone cement properties.* Clinical Orthopaedics and Related Research (1976-2007), 1997. **334**: p. 326-334.

23. Lewis, G., *Effect of mixing method and storage temperature of cement constituents on the fatigue and porosity of acrylic bone cement.* Journal of Biomedical Materials Research: An Official Journal of The Society for Biomaterials, The Japanese Society for Biomaterials, and The Australian Society for Biomaterials, 1999. **48**(2): p. 143-149.
24. Muller, S.D., S.M. Green, and A.W. McCaskie, *The dynamic volume changes of polymerising polymethyl methacrylate bone cement.* Acta orthopaedica Scandinavica, 2002. **73**(6): p. 684-687.
25. Wang, J.S., et al., *Is there any difference between vacuum mixing systems in reducing bone cement porosity?* Journal of Biomedical Materials Research: An Official Journal of The Society for Biomaterials and The Japanese Society for Biomaterials, 1996. **33**(2): p. 115-119.
26. Wang, J.-S., et al., *Porosity of bone cement reduced by mixing and collecting under vacuum.* Acta orthopaedica Scandinavica, 1993. **64**(2): p. 143-146.
27. Cox, B.D., et al., *Assessment of a three-dimensional measurement technique for the porosity evaluation of PMMA bone cement.* Journal of materials science. Materials in medicine, 2006. **17**(6): p. 553-557.
28. Kim, S., et al., *Influence of Porosity on Fracture Toughness and Fracture Behavior of Antibiotic-Loaded PMMA Bone Cement.* Journal of biomechanical engineering, 2022. **144**(1).
29. Nelson, R.C., R.O. Hoffman, and T.A. Burton, *The effect of antibiotic additions on the mechanical properties of acrylic cement.* Journal of biomedical materials research, 1978. **12**(4): p. 473-490.
30. Weisman, D.L., M.L. Olmstead, and J.J. Kowalski, *In Vitro Evaluation of Antibiotic Elution from Polymethylmethacrylate (PMMA) and Mechanical Assessment of Antibiotic-PMMA Composites.* Veterinary surgery, 2000. **29**(3): p. 245-251.
31. He, Y., et al., *Effect of antibiotics on the properties of poly(methylmethacrylate)-based bone cement.* Journal of biomedical materials research, 2002. **63**(6): p. 800-806.
32. Tuzuner, T., et al., *Elution characteristics and mechanical properties of calcium sulfate-loaded bone cement containing teicoplanin.* Journal of orthopaedic science : official journal of the Japanese Orthopaedic Association, 2007. **12**(2): p. 170-177.
33. Dunne, N., et al., *In vitro study of the efficacy of acrylic bone cement loaded with supplementary amounts of gentamicin: Effect on mechanical properties, antibiotic release, and biofilm formation.* Acta orthopaedica, 2007. **78**(6): p. 774-785.
34. Dunne, N.J., et al., *Incorporation of large amounts of gentamicin sulphate into acrylic bone cement: Effect on handling and mechanical properties, antibiotic release, and biofilm formation.* Proceedings of the Institution of Mechanical Engineers. Part H, Journal of engineering in medicine, 2008. **222**(3): p. 355-365.
35. Pelletier, M.H.M., et al., *The Compressive Properties of Bone Cements Containing Large Doses of Antibiotics.* The Journal of arthroplasty, 2009. **24**(3): p. 454-460.
36. Brock, H.S.M.D., et al., *Compression Strength and Porosity of Single-Antibiotic Cement Vacuum-Mixed With Vancomycin.* The Journal of arthroplasty, 2010. **25**(6): p. 990-997.
37. Kim, S., et al., *Mechanical effects, antimicrobial efficacy and cytotoxicity of usnic acid as a biofilm prophylaxis in PMMA.* Journal of materials science. Materials in medicine, 2011. **22**(12): p. 2773-2780.

38. Duey, R.E., et al., *Mechanical properties and elution characteristics of polymethylmethacrylate bone cement impregnated with antibiotics for various surface area and volume constructs.* The Iowa orthopaedic journal, 2012. **32**: p. 104-115.
39. Slane, J.A., et al., *The influence of low concentrations of a water soluble poragen on the material properties, antibiotic release, and biofilm inhibition of an acrylic bone cement.* Materials Science & Engineering C, 2014. **42**: p. 168-176.
40. Paz, E.M.D., et al., *Evaluation of Elution and Mechanical Properties of High-Dose Antibiotic-Loaded Bone Cement: Comparative "In Vitro" Study of the Influence of Vancomycin and Cefazolin.* The Journal of arthroplasty, 2015. **30**(8): p. 1423-1429.
41. Lee, S.-H., et al., *Elution and mechanical strength of vancomycin-loaded bone cement: In vitro study of the influence of brand combination.* PloS one, 2016. **11**(11): p. e0166545-e0166545.
42. Bishop, A.R., et al., *Vancomycin elution, activity and impact on mechanical properties when added to orthopedic bone cement.* Journal of the mechanical behavior of biomedical materials, 2018. **87**: p. 80-86.
43. Gandomkarzadeh, M., H.R. Moghimi, and A. Mahboubi, *Evaluation of the Effect of Ciprofloxacin and Vancomycin on Mechanical Properties of PMMA Cement; a Preliminary Study on Molecular Weight.* Scientific reports, 2020. **10**(1): p. 3981-3981.
44. Kim, S., et al., *Mechanical, elution, and antibacterial properties of simplex bone cement loaded with vancomycin.* Journal of the Mechanical Behavior of Biomedical Materials, 2020. **103**: p. 103588.
45. Lunz, A., et al., *Mechanical strength of antibiotic-loaded PMMA spacers in two-stage revision surgery.* BMC musculoskeletal disorders, 2022. **23**(1): p. 1-945.
46. Klekamp, J., et al., *The use of vancomycin and tobramycin in acrylic bone cement: Biomechanical effects and elution kinetics for use in joint arthroplasty.* The Journal of arthroplasty, 1999. **14**(3): p. 339-346.
47. Yousefsani, S.A., F. Farahmand, and A. Shamloo, *A three-dimensional micromechanical model of brain white matter with histology-informed probabilistic distribution of axonal fibers.* Journal of the mechanical behavior of biomedical materials, 2018. **88**: p. 288-295.
48. Macaulay, W., et al., *Differences in bone–cement porosity by vacuum mixing, centrifugation, and hand mixing.* The Journal of arthroplasty, 2002. **17**(5): p. 569-575.
49. Deluise, M. and C.P. Scott, *Addition of hand-blended generic tobramycin in bone cement: effect on mechanical strength*. 2004, SLACK Incorporated Thorofare, NJ. p. 1289-1291.
50. Lewis, G., S. Janna, and A. Bhattaram, *Influence of the method of blending an antibiotic powder with an acrylic bone cement powder on physical, mechanical, and thermal properties of the cured cement.* Biomaterials, 2005. **26**(20): p. 4317-4325.
51. Topoleski, L.D.T. and R. Rodriguez-Pinto, *7.2 Bone Cement, Editor(s): Paul Ducheyne,* Comprehensive Biomaterials II, Elsevier, 2017. p. 12-33.
52. Lewis, G., et al., *Influence of the radiopacifier in an acrylic bone cement on its mechanical, thermal, and physical properties: Barium sulfate-containing cement versus iodine-containing cement.* Journal of biomedical materials research. Part B, Applied biomaterials, 2005. **73B**(1): p. 77-87.

Highlights:

- Bone cement with a larger added antibiotic content has a higher porosity
- Three-parameter Weibull PDF can describe bone cement's pore distribution
- Elution of added antibiotic produces 0.5 to 1 mm micropores mainly
- Diverse fatigue test results might be explained by dissimilar pore distributions

Declaration of interests

☒ The authors declare that they have no known competing financial interests or personal relationships that could have appeared to influence the work reported in this paper.

☐The authors declare the following financial interests/personal relationships which may be considered as potential competing interests: